Research Paper

Three Models of a Sandwich Beam: Bending, Buckling, and Free Vibrations

Krzysztof MAGNUCKI[1)], Ewa MAGNUCKA-BLANDZI[2)], Leszek WITTENBECK[2)*]

[1)] *Łukasiewicz Research Network – Poznań Institute of Technology, Rail Vehicles Center*
Poznan, Poland

[2)] *Poznan University of Technology, Institute of Mathematics*
Poznan, Poland

*Corresponding Author e-mail: leszek.wittenbeck@put.poznan.pl

This paper is devoted to the analytical modelling of a sandwich beam. Three models of this beam are elaborated. Two nonlinear individual shear theories of deformation of a plane cross-sections are proposed. Based on Hamilton's principle, two differential equations of motion for each model are obtained. The bending, buckling and free flexural vibration problems of the simply-supported sandwich beam considering these three models are studied. The results of these analytical investigations are presented in tables.

Key words: shear deformation theory; deflection; critical load; fundamental natural frequency.

NOTATIONS

x, y, z – Cartesian coordinates,
L – length of the beam,
b – width of the beam,
h – total depth of the beam,
h_f – thicknesses of the faces,
h_c – thickness of the core,
$\chi_c = h_c/h$ – relative thickness of the core,
$u_f(x,t)$ – displacement of outer surfaces of the beam,
$\psi_f(x,t) = u_f(x,t)/h$ – dimensionless function,
$v(x,t)$ – deflection of the beam,
t – time,
$\eta = y/h$ – dimensionless coordinate,
$\xi = x/L$ – dimensionless coordinate,
E_f, E_c – Young's modulus of the faces and core, respectively,

ν_f, ν_c –   Poisson's ratio of the faces and core, respectively,

ρ_f, ρ_c –   mass density of the faces and core, respectively,

ρ_b –   mass density of the beam,

F –   force-load of three-point bending of the beam,

F_o –   axial force-load of the beam,

$\lambda = L/h$ –   relative length of the beam,

$\overline{v}_{\max}$ –   dimensionless maximal deflection,

$\overline{F}_{o,CR}$ –   dimensionless critical force,

f_z –   fundamental natural frequency,

$C_{se,b}$ –   shear coefficient in the three-point bending,

$C_{se,CR}$ –   shear coefficient in the buckling.

1. Introduction

Analytical modelling of the sandwich structures was initiated in the mid-20th century. The theoretical foundation and governing differential equations describing sandwich structure behaviour were presented in detail by Plantema [1] and Allen [2]. Noor *et al.* [3] focused on the review of computational models for sandwich plates and shells. Frostig [4] carried out a rigorous general stability analysis for some typical sandwich constructions subjected to in-plane external loads. Vinson [5] provided a general introduction to the structural mechanics in the field of sandwich structures and a sufficient number of references. Icardi [6] developed a sublaminate model for the analysis of sandwich beams with laminated faces, which incorporated a zig-zag representation of displacements within each sublaminate. Steeves and Fleck [7] considered the collapse strength of sandwich beams with composite face sheets and polymer foam cores. It was shown that the optimal designs for composite-polymer foam sandwich beams are of comparable weight to sandwich beams with metallic faces and a metallic foam core. Yang and Qiao [8] presented a higher-order sandwich impact theory and conducted a detailed study on the free vibration as well as the foreign object impact problem of a sandwich beam with a soft core. Magnucka-Blandzi and Magnucki [9] generalized the classical hypothesis of "broken line" to describe displacements in the three-layered beams with the core of varying properties. The strength and stability analyses were also conducted. Carrera and Brischetto [10] compared different theories to consider sandwich structures' bending and vibration problems. A brief survey of significant review papers and the latest developments on sandwich structure modelling were also given. Kreja [11] provided a state-of-the-art review on the computational treatment of laminated composite and sandwich panels. Magnucka-Blandzi [12] analysed a simply-supported sandwich beams with a metal foam core with mechanical properties that were varied in a normal direction in relation to the middle symmetry plane. The fields of displacement for the beam's flat cross section were

defined by three different hypotheses. Based on Hamilton's principle, the system of three partial differential equations of motion was obtained for each hypothesis and approximately solved. The subject of MAGNUCKA-BLANDZI' research [13] was a simply-supported rectangular sandwich plate with a core made of metal foam with properties varying across its thickness. The non-linear hypothesis of the field of displacements that is a generalisation of the classical hypotheses was assumed. The system of differential equations was formulated and approximately solved. Critical loads for a family of sandwich plates were numerically determined.

BABA [14] contributed towards the improvement of designing structures made from sandwich composites. His work dealt with the vibration behaviour of sandwich beams made of fibre-glass laminate skins wrapped over a polyurethane foam core. Experimental and numerical investigations on the natural frequencies of both flat and curved beams with and without debond were carried out. Results indicated that fundamental natural frequencies were seriously affected by curvature angle and debond, whereas the higher order natural frequencies showed relatively small changes. In PHAN *et al.* [15], a new one-dimensional high-order theory for orthotropic elastic sandwich beams was formulated. This theory was an extension of the high-order sandwich panel theory (HSAPT) and included the in-plane rigidity of the core. These results were compared with the corresponding ones from the elasticity solution. Furthermore, the results using the classical sandwich model without shear, the first-order shear, and the earlier HSAPT were also presented for completeness. The comparison among these numerical results showed that the solution from the current theory was very close to that of the elasticity in terms of both the displacements and stress or strains, especially the shear stress distributions in the core for a wide range of cores.

In MAGNUCKI *et al.* [16], the strength and buckling problem of a five-layer sandwich beam under axial compression or bending was presented. A mathematical model of the field of displacements, which includes shear effect and bending moment, was developed. The system of partial differential equations of equilibrium for the five-layer sandwich beam was derived on the basis of the principle of stationary total potential energy and analytically solved. SAYYAD and GHUGAL [17] undertook an extensive review of the literature available for the bending, free vibration and buckling analysis of laminated composite and sandwich beams. In MAGNUCKA-BLANDZI [18], an original mathematical model of seven-layer beams was formulated. Based on the principle of the total potential energy, the equations of equilibrium were derived and analytically solved. The deflections and the critical axial force were determined for different values of the trapezoidal corrugation pitch of the main core. CZECHOWSKI *et al.* [19] dealt with an experimental investigation of the mechanical properties of sandwich beams obtained from bending tests. The tested specimens consisted of

foam or honeycomb core and face sheets made of aluminium alloys, plywood or composite material. The face sheets and the core were bonded with glue material. Beams of different dimensions, namely beam width, core and face sheets thickness, were tested. Three-point bending tests were carried out, in which the beam's mid-span deflections versus applied force were recorded. Experimental test results were compared with simulations on the basis of the finite element method. BIRMAN and KARDOMATEAS [20] outlined the review of the papers on sandwich structures and concentrated on the theoretical models and applications of such structures and observations of their behaviour under a multitude of loads. SAYYAD and GHUGAL [21] focused on the review of literature on bending, buckling, and vibration analysis of functionally graded sandwich beams under mechanical and thermal loads using elasticity theory, analytical methods, and numerical methods based on classical and refined shear deformation theories.

In ZHEN *et al.* [22], a Reddy-type higher-order zig-zag model was proposed for the critical load analysis of laminated composite and sandwich beams. The proposed model can describe the discontinuity of the slope of the in-plane displacement at the interface using the zig-zag function, and satisfies the interlaminar continuity condition of transverse shear stresses at interfaces using the three-field Hu-Washizu mixed variational principle. Laminated composite and sandwich beams with various configurations including material properties, length-to-thickness and lay-ups were taken into account. Numerical results were compared with those computed by other models to show the agreement of the proposed model. MAGNUCKI [23] analysed the bending problems of sandwich beams and I-beams with consideration of the shear effect. Based on the principle of stationary total potential energy, the differential equations of equilibrium were obtained. The system of the equations was analytically solved for two types of load: three-point bending and uniformly distributed load. MAGNUCKI and MAGNUCKA-BLANDZI [24] provided a generalisation of the analytical model of sandwich structures. The individual nonlinear theory of deformation of the straight line normal to the neutral surface was developed. This analytical model of sandwich structures was presented in detail for the exemplary rectangular plate. Based on the principle of stationary potential energy, differential equations of equilibrium of the plate were obtained and analytically solved.

The main goal of this paper is to present three models of the simply-supported sandwich beam of the total depth h, width b and length L. The beam is under three-point bending force F or axial compression force F_o (Fig. 1).

The novelty of this paper lies in the use of an efficient shear theory [24] for the sandwich beam. The three analytical models of the sandwich beam are analysed. The first model is formulated as the classical sandwich beam with consideration of the "broken line" theory. The second model is a generalisation of the first model; the nonlinear shear effect in the core is only considered. In
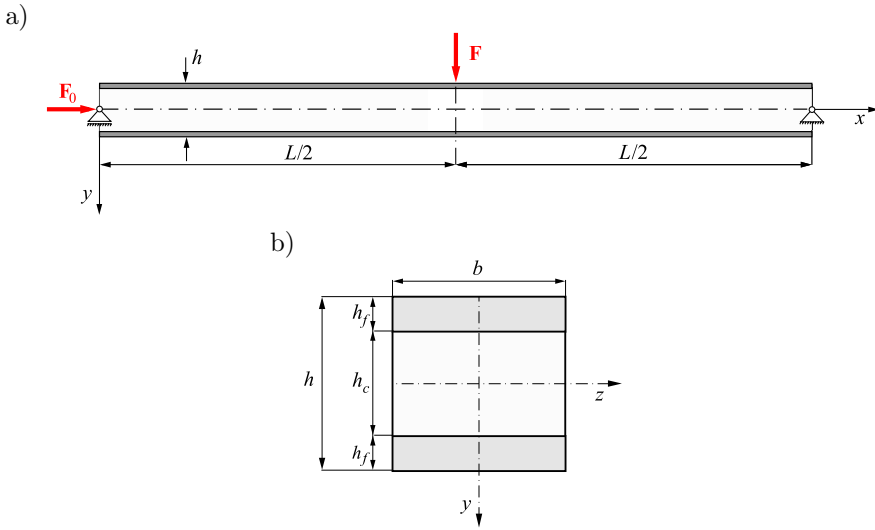
a)

b)

FIG. 1. Schemes: a) loads of the sandwich beam, b) the cross-section of the beam.

the third model, the nonlinear shear effect in the faces and the core is taken into account. The deflections, elastic buckling and flexural free vibrations of exemplary simply-supported beams for each model are analytically determined and compared with the FEM results using ABAQUS software.

2. THE FIRST MODEL – THE LINEAR SHEAR EFFECT ONLY IN THE CORE

The deformation of a planar cross-section of the sandwich beam in accordance with the "broken line" theory – the classical model is shown in Fig. 2.
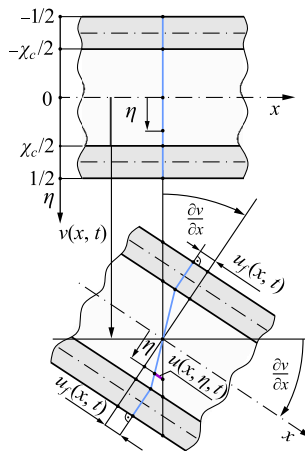

FIG. 2. Deformation scheme of the beam's planar cross-section – the classical model.

The longitudinal displacements in accordance with Fig. 2 are as follows:
- the upper face ($-1/2 \leq \eta \leq -\chi_c/2$)

$$(2.1) \qquad u(x, \eta, t) = -h \left[\eta \frac{\partial v}{\partial x} + \psi_f(x, t) \right],$$

- the core ($-\chi_c/2 \leq \eta \leq \chi_c/2$)

$$(2.2) \qquad u(x, \eta, t) = -h\eta \left[\frac{\partial v}{\partial x} - \frac{2}{\chi_c} \psi_f(x, t) \right],$$

- the lower face ($\chi_c/2 \leq \eta \leq 1/2$)

$$(2.3) \qquad u(x, \eta, t) = -h \left[\eta \frac{\partial v}{\partial x} - \psi_f(x, t) \right],$$

where $\psi_f(x, t) = u_f(x, t)/h$ – dimensionless displacement function, $\chi_c = h_c/h$ – relative thickness of the core, $\eta = y/h$ – dimensionless coordinate, $v(x, t)$ – deflection of the beam, t – time.

Therefore, the strains are in the following form:
- the upper/lower faces

$$(2.4) \qquad \begin{aligned} \varepsilon_x^{(uf)}(x, \eta, t) &= -h \left[\eta \frac{\partial^2 v}{\partial x^2} + \frac{\partial \psi_f}{\partial x} \right], \\ \varepsilon_x^{(lf)}(x, \eta, t) &= -h \left[\eta \frac{\partial^2 v}{\partial x^2} - \frac{\partial \psi_f}{\partial x} \right], \end{aligned}$$

$$(2.5) \qquad \gamma_{xy}^{(uf)}(x, t) = \gamma_{xy}^{(lf)}(x, t) = 0,$$

- the core

$$(2.6) \qquad \varepsilon_x^{(c)}(x, \eta, t) = -h\eta \left[\frac{\partial^2 v}{\partial x^2} - \frac{2}{\chi_c} \frac{\partial \psi_f}{\partial x} \right], \qquad \gamma_{xy}^{(c)}(x, t) = \frac{2}{\chi_c} \psi_f(x, t).$$

Consequently, the stresses (Hooke's law) are in the following form:
- the upper/lower faces

$$(2.7) \qquad \sigma_x^{(uf)}(x, \eta, t) = E_f \varepsilon_x^{(uf)}(x, \eta, t), \qquad \sigma_x^{(lf)}(x, \eta, t) = E_f \varepsilon_x^{(lf)}(x, \eta, t),$$

$$(2.8) \qquad \tau_{xy}^{(uf)}(x, t) = \tau_{xy}^{(lf)}(x, t) = 0,$$

where E_f is Young's modulus of the faces.

- the core

$$\sigma_x^{(c)}(x, \eta, t) = E_c \varepsilon_x^{(c)}(x, \eta, t),$$

(2.9)

$$\tau_{xy}^{(c)}(x, t) = \frac{E_c}{2(1 + \nu_c)} \gamma_{xy}^{(c)}(x, t),$$

where E_c, ν_c are Young's modulus and Poisson's ratio of the core, respectively.

The bending moment is

$$(2.10) \qquad M_b(x, t) = bh^2 \left\{ \int\limits_{-1/2}^{-\chi_c/2} \eta \sigma_x^{(uf)}(x, \eta, t) \, \mathrm{d}\eta + \int\limits_{-\chi_c/2}^{\chi_c/2} \eta \sigma_x^{(c)}(x, \eta, t) \, \mathrm{d}\eta \right.$$

$$\left. + \int\limits_{\chi_c/2}^{1/2} \eta \sigma_x^{(lf)}(x, \eta, t) \, \mathrm{d}\eta \right\}.$$

Substituting the expressions (2.7) and (2.9) for normal stresses and integrating, one obtains the following equation:

$$(2.11) \qquad C_{vv1} \frac{\partial^2 v}{\partial x^2} - C_{v\psi1} \frac{\partial \psi_f}{\partial x} = -12 \frac{M_b(x, t)}{E_f bh^3},$$

where $C_{vv1} = 1 - (1 - e_c)\chi_c^3$, $C_{v\psi1} = 3 - (3 - 2e_c)\chi_c^2$, $e_c = E_c/E_f$ are dimensionless coefficients.

The elastic strain energy of the beam is

$$(2.12) \quad U_\varepsilon = \frac{1}{2} E_f bh \int\limits_0^L \left\{ \int\limits_{-1/2}^{-\chi_c/2} \left(\varepsilon_x^{(uf)}(x, \eta, t) \right)^2 \, \mathrm{d}\eta \right.$$

$$+ e_c \int\limits_{-\chi_c/2}^{\chi_c/2} \left[\left(\varepsilon_x^{(c)}(x, \eta, t) \right)^2 + \frac{1}{2(1 + \nu_c)} \left(\gamma_{xy}^{(c)}(x, t) \right)^2 \right] \mathrm{d}\eta$$

$$\left. + \int\limits_{\chi_c/2}^{1/2} \left(\varepsilon_x^{(lf)}(x, \eta, t) \right)^2 \, \mathrm{d}\eta \right\} \mathrm{d}x.$$

Taking into account the expressions (2.4) and (2.6), one obtains

$$(2.13) \quad U_\varepsilon = \frac{E_f bh^3}{24} \int\limits_0^L \left\{ C_{vv1} \left(\frac{\partial^2 v}{\partial x^2} \right)^2 - 2C_{v\psi1} \frac{\partial^2 v}{\partial x^2} \frac{\partial \psi_f}{\partial x} \right.$$

$$\left. + C_{\psi\psi1} \left(\frac{\partial \psi_f}{\partial x} \right)^2 + C_{\psi1} \frac{\psi_f^2(x,t)}{h^2} \right\} \mathrm{d}x,$$

where

$$C_{\psi\psi1} = 4\left[3 - (3 - e_c)\chi_c\right] \qquad \text{and} \qquad C_{\psi1} = \frac{24}{1 + \nu_c} \frac{e_c}{\chi_c}$$

are dimensionless coefficients.

The work of the load is

$$(2.14) \qquad W = \int\limits_0^L \left\{ T(x) \frac{\partial v}{\partial x} + \frac{1}{2} F_o \left(\frac{\partial v}{\partial x} \right)^2 \right\} \mathrm{d}x,$$

where $T(x)$ is the transverse force, and F_o is the axial compressive force.

The kinetic energy of the beam is

$$(2.15) \qquad U_k = \frac{1}{2} \rho_b bh \int\limits_0^L \left(\frac{\partial v}{\partial t} \right)^2 \mathrm{d}x,$$

where $\rho_b = (1 - \chi_c)\rho_f + \chi_c \rho_c$ is the mass density of the beam, and ρ_f, ρ_c are the mass density of the faces and core, respectively.

Based on Hamilton's principle

$$(2.16) \qquad \delta \int\limits_{t_1}^{t_2} [U_k - (U_\varepsilon - W)] \, \mathrm{d}t = 0,$$

two differential equations of motion are obtained in the following form:

$$(2.17) \quad \rho_b bh \frac{\partial^2 v}{\partial t^2} + \frac{1}{12} E_f bh^3 \left(C_{vv1} \frac{\partial^4 v}{\partial x^4} - C_{v\psi1} \frac{\partial^3 \psi_f}{\partial x^3} \right) + \frac{\mathrm{d}T}{\mathrm{d}x} + F_o \frac{\partial^2 v}{\partial x^2} = 0,$$

$$(2.18) \qquad C_{v\psi1} \frac{\partial^3 v}{\partial x^3} - C_{\psi\psi1} \frac{\partial^2 \psi_f}{\partial x^2} + C_{\psi1} \frac{\psi_f(x,t)}{h^2} = 0.$$

It may be easily noticed, that first Eq. (2.17) of this system and Eq. (2.11) are equivalent for the static problems. Thus, Eqs. (2.11) and (2.18) are governing equilibrium equations of the bending and buckling of sandwich beams.

2.1. Three-point bending of the beam

The bending moment of the beam is

(2.19)
$$M_b(x) = \frac{1}{2}Fx, \qquad 0 \leq x \leq L/2,$$

where F is the concentrated force at the midpoint of the beam.

Therefore, the system of two equations of equilibrium (2.11) and (2.18) is as follows:

(2.20)
$$C_{vv1}\frac{\mathrm{d}^2 v}{\mathrm{d}x^2} - C_{v\psi1}\frac{\mathrm{d}\psi_f}{\mathrm{d}x} = -6x\frac{F}{E_f bh^3},$$

$$C_{v\psi1}\frac{\mathrm{d}^3 v}{\mathrm{d}x^3} - C_{\psi\psi1}\frac{\mathrm{d}^2\psi_f}{\mathrm{d}x^2} + C_{\psi1}\frac{\psi_f(x)}{h^2} = 0.$$

This system, after simple transformation, is reduced to one differential equation:

(2.21)
$$\frac{\mathrm{d}^2\psi_f}{\mathrm{d}\xi^2} - (k_1\lambda)^2\,\psi_f(\xi) = -6\frac{C_{v\psi1}}{C_{vv1}C_{\psi\psi1} - C_{v\psi1}^2}\lambda^2\frac{F}{E_f bh},$$

where $k_1 = \sqrt{\dfrac{C_{vv1}C_{\psi1}}{C_{vv1}C_{\psi\psi1} - C_{v\psi1}^2}}$ is the dimensionless coefficient, $\lambda = L/h$ is relative length, and $\xi = x/L$ is the dimensionless coordinate ($0 \leq \xi \leq 1/2$).

The solution of this equation is the following function:

(2.22)
$$\psi_f(\xi) = 6\left[1 - \frac{\cosh(k_1\lambda\xi)}{\cosh(k_1\lambda/2)}\right]\frac{C_{v\psi1}}{C_{vv1}C_{\psi1}}\frac{F}{E_f bh}.$$

This function satisfies the following conditions: $\mathrm{d}\psi_f/\mathrm{d}\xi|_0 = 0$ and $\psi_f(1/2) = 0$.

Therefore, the maximum relative deflection of the beam based on the first equation of the system (2.20), with consideration of the conditions $v(0) = 0$ and $\mathrm{d}v/\mathrm{d}\xi|_{1/2} = 0$, is as follows:

(2.23)
$$\widetilde{v}_{\max}^{(1)} = \frac{v(1/2)}{L} = \overline{v}_{\max}^{(1)}\frac{F}{E_f bh},$$

where the dimensionless maximal deflection is

(2.24)
$$\overline{v}_{\max}^{(1)} = \left(1 + C_{se,b}^{(1)}\right)\frac{\lambda^2}{4C_{vv1}},$$

and the shear coefficient in the three-point bending is

(2.25) $$C_{se,b}^{(1)} = \frac{12}{\lambda^2}\left[1 - \frac{2}{k_1\lambda}\tanh\left(\frac{1}{2}k_1\lambda\right)\right]\frac{C_{v\psi1}^2}{C_{vv1}C_{\psi1}}.$$

Moreover, the shear stresses are:

- the upper/lower faces

(2.26) $$\tau_{xy}^{(1,f)}(\xi,\eta) = \overline{\tau}_{xy}^{(1,f)}(\xi,\eta) = 0,$$

- the core

(2.27) $$\tau_{xy}^{(1,c)}(\xi,\eta) = \overline{\tau}_{xy}^{(1,c)}(\xi,\eta)\frac{F}{bh},$$

where the dimensionless shear stress is

(2.28) $$\overline{\tau}_{xy}^{(1,c)}(\xi,\eta) = \frac{6}{1+\nu_c}\frac{e_0}{\chi_c}\left[1 - \frac{\cosh(k_1\lambda\xi)}{\cosh(k_1\lambda/2)}\right]\frac{C_{v\psi1}}{C_{vv1}C_{\psi1}}.$$

2.2. Elastic buckling of the beam

The bending moment of the simply-supported buckled beam:

(2.29) $$M_b(x) = F_o v(x), \qquad 0 \le x \le L.$$

Therefore, the system of two equations of equilibrium (2.11) and (2.18) is as follows:

(2.30)
$$C_{vv1}\frac{\mathrm{d}^2 v}{\mathrm{d}x^2} - C_{v\psi1}\frac{\mathrm{d}\psi_f}{\mathrm{d}x} + 6v(x)\frac{F_o}{E_f bh^3} = 0,$$

$$C_{v\psi1}\frac{\mathrm{d}^3 v}{\mathrm{d}x^3} - C_{\psi\psi1}\frac{\mathrm{d}^2\psi_f}{\mathrm{d}x^2} + C_{\psi1}\frac{\psi_f(x)}{h^2} = 0.$$

This system is approximately solved with the use of two assumed functions:

(2.31) $$v(x) = v_a \sin\left(\pi\frac{x}{L}\right), \qquad \psi_f(x) = \psi_a \cos\left(\pi\frac{x}{L}\right),$$

where v_a, ψ_a are the parameters of the functions.

These functions satisfy the conditions of a simply-supported beam. Substituting these functions (2.31) into Eqs. (2.30), one obtains the homogeneous system of algebraic equations:

(2.32)
$$\left[\left(\frac{\pi}{L}\right)^2 C_{vv1} - 12\frac{F_o}{E_f bh^3}\right]v_a - \frac{\pi}{L}C_{v\psi1}\psi_a = 0,$$

$$\frac{\pi}{L}C_{v\psi1}v_a - \left[C_{\psi\psi1} + \frac{\lambda^2}{\pi^2}C_{\psi1}\right]\psi_a = 0,$$

from which the critical force is

$$(2.33) \qquad F_{o,CR}^{(1)} = \overline{F}_{o,CR}^{(1)} E_f bh,$$

where the dimensionless critical force is

$$(2.34) \qquad \overline{F}_{o,CR}^{(1)} = \left(1 - C_{se,CR}^{(1)}\right) \frac{\pi^2 C_{vv1}}{12\lambda^2},$$

and the shear coefficient in the buckling is

$$(2.35) \qquad C_{se,CR}^{(1)} = \frac{\pi^2}{\pi^2 C_{\psi\psi1} + \lambda^2 C_{\psi1}} \frac{C_{v\psi1}^2}{C_{vv1}}.$$

2.3. Free flexural vibration of the beam

The system of two differential equations of motion (2.17) and (2.18) for the free flexural vibration of the simply-supported sandwich beam is in the following form:

$$(2.36)$$
$$\rho_b bh \frac{\partial^2 v}{\partial t^2} + \frac{1}{12} E_f bh^3 \left(C_{vv1} \frac{\partial^4 v}{\partial x^4} - C_{v\psi1} \frac{\partial^3 \psi_f}{\partial x^3} \right) = 0,$$

$$C_{v\psi1} \frac{\partial^3 v}{\partial x^3} - C_{\psi\psi1} \frac{\partial^2 \psi_f}{\partial x^2} + C_{\psi1} \frac{\psi_f(x,t)}{h^2} = 0.$$

This system is approximately solved with the use of two assumed functions:

$$(2.37) \qquad v(x,t) = v_a(t) \sin\left(\pi \frac{x}{L}\right), \qquad \psi_f(x,t) = \psi_a(t) \cos\left(\pi \frac{x}{L}\right),$$

where $v_a(t)$, $\psi_a(t)$ are the functions of time t.

Substituting these functions (2.37) into Eqs. (2.36), and after simple transformation, one obtains the following equation:

$$(2.38) \qquad \frac{d^2 v_a}{dt^2} + \left(1 - C_{se,fv}^{(1)}\right) \frac{\pi^4 C_{vv1}}{12\lambda^4} \frac{E_f}{\rho_b h^2} v_a(t) = 0,$$

where the shear coefficient in the free flexural vibration is

$$(2.39) \qquad C_{se,fv}^{(1)} = \frac{\pi^2}{\pi^2 C_{\psi\psi1} + \lambda^2 C_{\psi1}} \frac{C_{v\psi1}^2}{C_{vv1}}.$$

This shear coefficient is identical as in the buckling problem (2.35).

Equation (2.38) is approximately solved with the use of the function

$$(2.40) \qquad v_a(t) = v_a \sin(\omega t),$$

where v_a [mm] is the amplitude of the flexural vibration, and ω [1/s] is the fundamental natural frequency.

Substituting this function into Eq. (2.38), after simple transformation, one obtains the fundamental natural frequency:

$$(2.41) \qquad f_z^{(1)} = \frac{\omega^{(1)}}{2\pi} = \frac{\sqrt{3}\pi^2 10^6}{6\lambda^2} \sqrt{\left(1 - C_{se,fv}^{(1)}\right) C_{vv1} \frac{E_f}{\rho_b h^2}} \ \ [\text{Hz}],$$

where dimensions of quantities are: E_f [MPa], ρ_b [kg/m^3], and h [mm].

3. THE SECOND MODEL – THE NONLINEAR SHEAR EFFECT IN THE CORE

The deformation of a planar cross-section after the beam's bending is shown in Fig. 3.
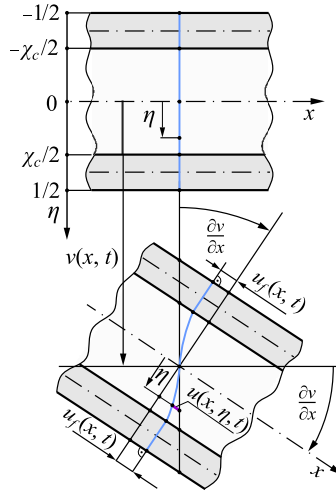

FIG. 3. Deformation scheme of the beam's planar cross-section – the second model.

The longitudinal displacements in accordance with Fig. 3 are as follows:
- the upper face $(-1/2 \leq \eta \leq -\chi_c/2)$

$$(3.1) \qquad u(x,\eta,t) = -h\left[\eta\frac{\partial v}{\partial x} + \psi_f(x,t)\right],$$

- the core $(-\chi_c/2 \leq \eta \leq \chi_c/2)$

$$(3.2) \qquad u(x,\eta,t) = -h\left[\eta\frac{\partial v}{\partial x} - f_{d,c}^{(2)}(\eta)\psi_f(x,t)\right],$$

- the lower face ($\chi_c/2 \leq \eta \leq 1/2$)

$$(3.3) \qquad u(x, \eta, t) = -h \left[\eta \frac{\partial v}{\partial x} - \psi_f(x, t) \right],$$

where the dimensionless function of the deformation of a planar cross-section of the core, taking into account [18] and [19], is assumed in the following form:

$$(3.4) \qquad f_{d,c}^{(2)}(\eta) = 2 \frac{3 \left[1 - (1 - e_c)\chi_c^2 \right] \eta - 4e_c\eta^3}{\left[3 - (3 - 2e_c)\chi_c^2 \right] \chi_c}.$$

Therefore, the strains are in the following form:
- the upper/lower faces

$$(3.5) \qquad \begin{aligned} \varepsilon_x^{(uf)}(x, \eta, t) &= -h \left[\eta \frac{\partial^2 v}{\partial x^2} + \frac{\partial \psi_f}{\partial x} \right], \\ \varepsilon_x^{(lf)}(x, \eta, t) &= -h \left[\eta \frac{\partial^2 v}{\partial x^2} - \frac{\partial \psi_f}{\partial x} \right], \end{aligned}$$

$$(3.6) \qquad \gamma_{xy}^{(uf)}(x, t) = \gamma_{xy}^{(lf)}(x, t) = 0,$$

- the core

$$(3.7) \qquad \begin{aligned} \varepsilon_x^{(c)}(x, \eta, t) &= -h \left[\eta \frac{\partial^2 v}{\partial x^2} - f_{d,c}^{(2)}(\eta) \frac{\partial \psi_f}{\partial x} \right], \\ \gamma_{xy}^{(c)}(x, \eta, t) &= \frac{\mathrm{d} f_{d,c}^{(2)}}{\mathrm{d}\eta} \psi_f(x, t). \end{aligned}$$

Therefore, Eq. (2.11) and two equations of motion (2.17) and (2.18) for the second model are as follows:

$$(3.8) \qquad C_{vv2} \frac{\partial^2 v}{\partial x^2} - C_{v\psi2} \frac{\partial \psi_f}{\partial x} = -12 \frac{M_b(x, t)}{E_f b h^3},$$

and two differential equations of motion are:

$$(3.9) \qquad \rho_b b h \frac{\partial^2 v}{\partial t^2} + \frac{1}{12} E_f b h^3 \left(C_{vv2} \frac{\partial^4 v}{\partial x^4} - C_{v\psi2} \frac{\partial^3 \psi_f}{\partial x^3} \right) + \frac{\mathrm{d}T}{\mathrm{d}x} + F_o \frac{\partial^2 v}{\partial x^2} = 0,$$

$$(3.10) \qquad C_{v\psi2} \frac{\partial^3 v}{\partial x^3} - C_{\psi\psi2} \frac{\partial^2 \psi_f}{\partial x^2} + C_{\psi2} \frac{\psi_f(x, t)}{h^2} = 0,$$

where

$$C_{vv2} = 1 - (1 - e_c)\chi_c^3,$$

$$C_{v\psi2} = 3\left[1 - \chi_c^2 + \frac{2}{5}\frac{5\left(1 - \chi_c^2\right) + 4e_c\chi_c^2}{3\left(1 - \chi_c^2\right) + 2e_c\chi_c^2}e_c\chi_c^2\right],$$

$$C_{\psi\psi2} = 12\left\{1 - \chi_c + \frac{105\left(1 - \chi_c^2\right)^2 + 168\left(1 - \chi_c^2\right)e_c\chi_c^2 + 68e_c^2\chi_c^4}{35\left[3\left(1 - \chi_c^2\right) + 2e_c\chi_c^2\right]^2}e_c\chi_c\right\},$$

$$C_{\psi2} = \frac{72}{1 + \nu_c}\frac{15\left(1 - \chi_c^2\right)^2 + 20\left(1 - \chi_c^2\right)e_c\chi_c^2 + 8e_c^2\chi_c^4}{5\left[3\left(1 - \chi_c^2\right) + 2e_c\chi_c^2\right]^2}\frac{e_c}{\chi_c}.$$

3.1. Three-point bending of the beam

Therefore, the maximal relative deflection of the beam (2.23) for the second model is as follows:

$$(3.11) \qquad \widetilde{v}_{\max}^{(2)} = \overline{v}_{\max}^{(2)}\frac{F}{E_f bh},$$

where the dimensionless maximal deflection is

$$(3.12) \qquad \overline{v}_{\max}^{(2)} = \left(1 + C_{se,b}^{(2)}\right)\frac{\lambda^2}{4C_{vv2}},$$

the shear coefficient in the three-point bending is

$$(3.13) \qquad C_{se,b}^{(2)} = \frac{12}{\lambda^2}\left[1 - \frac{2}{k_2\lambda}\tanh\left(\frac{1}{2}k_2\lambda\right)\right]\frac{C_{v\psi2}^2}{C_{vv2}C_{\psi2}},$$

and $k_2 = \sqrt{\dfrac{C_{vv2}C_{\psi2}}{C_{vv2}C_{\psi\psi2} - C_{v\psi2}^2}}$ is the dimensionless coefficient.

Moreover, the dimensionless shear stresses are:

- the upper/lower faces

$$(3.14) \qquad \overline{\tau}_{xy}^{(2,f)}(\xi, \eta) = 0,$$

- the core

$$(3.15) \qquad \overline{\tau}_{xy}^{(2,c)}(\xi, \eta) = \frac{18}{1 + \nu_c}\frac{1 - (1 - e_c)\chi_c^2 - 4e_c\eta^2}{3 - (3 - 2e_c)\chi_c^2}\frac{e_0}{\chi_c}$$

$$\cdot\left[1 - \frac{\cosh(k_2\lambda\xi)}{\cosh(k_2\lambda/2)}\right]\frac{C_{v\psi2}}{C_{vv2}C_{\psi2}}.$$

3.2. Elastic buckling of the beam

Thus, the critical force of the beam (2.33) for the second model is as follows:

$$(3.16) \qquad F_{o,CR}^{(2)} = \overline{F}_{o,CR}^{(2)} E_f bh,$$

where the dimensionless critical force is

$$(3.17) \qquad \overline{F}_{o,CR}^{(2)} = \left(1 - C_{se,CR}^{(2)}\right) \frac{\pi^2 C_{vv2}}{12\lambda^2},$$

and the shear coefficient in the buckling is

$$(3.18) \qquad C_{se,CR}^{(2)} = \frac{\pi^2}{\pi^2 C_{\psi\psi2} + \lambda^2 C_{\psi2}} \frac{C_{v\psi2}^2}{C_{vv2}}.$$

3.3. Free flexural vibration of the beam

Consequently, the fundamental natural frequency (2.41) for the second model is as follows:

$$(3.19) \qquad f_z^{(2)} = \frac{\omega^{(2)}}{2\pi} = \frac{\sqrt{3}\pi^2 10^6}{6\lambda^2} \sqrt{\left(1 - C_{se,fv}^{(2)}\right) C_{vv2} \frac{E_f}{\rho_b h^2}} \quad [\text{Hz}],$$

where the shear coefficient in the free flexural vibration $C_{se,fv}^{(2)} = C_{se,CR}^{(2)}$.

4. THE THIRD MODEL – THE NONLINEAR SHEAR EFFECT IN THE FACES AND THE CORE

The deformation of a planar cross-section after the beam's bending is shown in Fig. 4.

The longitudinal displacements in accordance with Fig. 4 are as follows:

• the upper face $(-1/2 \leq \eta \leq -\chi_c/2)$

$$(4.1) \qquad u(x, \eta, t) = -h \left[\eta \frac{\partial v}{\partial x} + f_{d,f}^{(3)}(\eta) \psi_f(x, t)\right],$$

• the core $(-\chi_c/2 \leq \eta \leq \chi_c/2)$

$$(4.2) \qquad u(x, \eta, t) = -h \left[\eta \frac{\partial v}{\partial x} - f_{d,c}^{(3)}(\eta) \psi_f(x, t)\right],$$
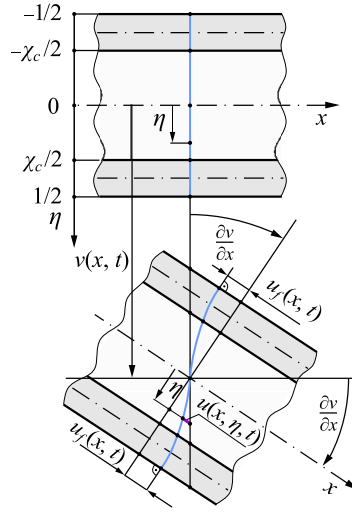
FIG. 4. Deformation scheme of the beam's planar cross-section – the third model.

- the lower face $(\chi_c/2 \leq \eta \leq 1/2)$

$$(4.3) \qquad u(x, \eta, t) = -h \left[\eta \frac{\partial v}{\partial x} - f_{d,f}^{(3)}(\eta) \psi_f(x, t) \right],$$

where the dimensionless functions of the deformation of a planar cross-section of the faces and the core, taking into account the expression (3.4), are assumed in the following form:

$$(4.4) \qquad f_{d,f}^{(3)}(\eta) = \frac{1}{1 + \beta}(\beta - 3\eta + 4\eta^3),$$

$$f_{d,c}^{(3)}(\eta) = \frac{C_0}{(1 + \beta)\chi_c} \left\{ 3 \left[1 - (1 - e_c)\chi_c^2 \right] \eta - 4e_c\eta^3 \right\},$$

and the coefficient $C_0 = \frac{2\beta + (3 - \chi_c^2)\chi_c}{3(1 - \chi_c^2) + 2e_c\chi_c^2}$ and the parameter β $(2 < \beta)$.

Therefore, the strains are in the following form:

- the upper/lower faces

$$(4.5) \qquad \varepsilon_x^{(uf)}(x, \eta, t) = -h \left[\eta \frac{\partial^2 v}{\partial x^2} + f_{d,f}^{(3)}(\eta) \frac{\partial \psi_f}{\partial x} \right],$$

$$\varepsilon_x^{(lf)}(x, \eta, t) = -h \left[\eta \frac{\partial^2 v}{\partial x^2} - f_{d,f}^{(3)}(\eta) \frac{\partial \psi_f}{\partial x} \right],$$

$$(4.6) \qquad \gamma_{xy}^{(uf)}(x, t) = \gamma_{xy}^{(lf)}(x, t) = \frac{3}{1 + \beta}(1 - 4\eta^2)\psi_f(x),$$

- the core

$$\varepsilon_x^{(c)}(x,\eta,t) = -h\eta \left[\frac{\partial^2 v}{\partial x^2} - f_{d,c}^{(3)}(\eta) \frac{\partial \psi_f}{\partial x} \right],$$

(4.7)

$$\gamma_{xy}^{(c)}(x,t) = \frac{\mathrm{d} f_{d,c}^{(3)}}{\mathrm{d}\eta} \psi_f(x,t).$$

Therefore, Eq. (2.11) and two equations of motion (2.17) and (2.18) for the third model are as follows:

(4.8) $$C_{vv3} \frac{\partial^2 v}{\partial x^2} - C_{v\psi3} \frac{\partial \psi_f}{\partial x} = -12 \frac{M_b(x,t)}{E_f b h^3},$$

and two differential equations of motion are:

(4.9) $$\rho_b b h \frac{\partial^2 v}{\partial t^2} + \frac{1}{12} E_f b h^3 \left(C_{vv3} \frac{\partial^4 v}{\partial x^4} - C_{v\psi3} \frac{\partial^3 \psi_f}{\partial x^3} \right) + \frac{\mathrm{d}T}{\mathrm{d}x} + F_o \frac{\partial^2 v}{\partial x^2} = 0,$$

(4.10) $$C_{v\psi3} \frac{\partial^3 v}{\partial x^3} - C_{\psi\psi3} \frac{\partial^2 \psi_f}{\partial x^2} + C_{\psi3} \frac{\psi_f(x,t)}{h^2} = 0,$$

where

$$C_{vv3} = 1 - (1 - e_c)\chi_c^3,$$

$$C_{v\psi3} = \frac{3}{5(1+\beta)} \left\{ 4 + 5\beta(1 - \chi_c^2) - (5 - \chi_c^2)\chi_c^3 + C_0 e_c \chi_c^2 \left[5(1 - \chi_c^2) + 4 e_c \chi_c^2 \right] \right\},$$

$$C_{\psi\psi3} = \frac{3}{35(1+\beta)^2}$$
$$\cdot \left\{ 68 + 35\beta \left[4\beta(1 - \chi_c^2) + 5 - (6 - \chi_c^2)\chi_c^2 \right] - \left(105 - 42\chi_c^2 + 5\chi_c^4 \right) \chi_c^3 \right.$$
$$\left. + C_0^2 e_c \chi_c \left[105(1 - \chi_c^2)^2 + 168 e_c \chi_c^2 (1 - \chi_c^2) + 68 e_c^2 \chi_c^4 \right] \right\},$$

$$C_{\psi3} = \frac{18}{5(1+\beta)^2} \left\{ \frac{1}{1+\nu_f} + \left(8 - 15\chi_c + 10\chi_c^3 - 3\chi_c^5 \right) \right.$$
$$\left. - \frac{C_0^2}{1+\nu_c} \frac{e_c}{\chi_c} \left[15 \left(1 - \chi_c^2 \right)^2 + 20 e_c \chi_c^2 \left(1 - \chi_c^2 \right) + 8 e_c^2 \chi_c^4 \right] \right\}.$$

4.1. Three-point bending of the beam

Therefore, the maximum relative deflection of the beam (2.23), for the third model, is

(4.11) $$\widetilde{v}_{\max}^{(3)} = \overline{v}_{\max}^{(3)} \frac{F}{E_f b h},$$

where the dimensionless maximal deflection is

$$(4.12) \qquad \overline{v}_{\max}^{(3)} = \left(1 + C_{se,b}^{(3)}\right) \frac{\lambda^2}{4C_{vv3}},$$

the shear coefficient in the three-point bending is

$$(4.13) \qquad C_{se,b}^{(3)} = \max_\beta \frac{12}{\lambda^2} \left[1 - \frac{2}{k_3\lambda} \tanh\left(\frac{1}{2}k_3\lambda\right)\right] \frac{C_{v\psi 3}^2}{C_{vv3}C_{\psi 3}},$$

and $k_3 = \sqrt{\frac{C_{vv3}C_{\psi 3}}{C_{vv3}C_{\psi\psi 3} - C_{v\psi 3}^2}}$ is the dimensionless coefficient.

Moreover, the dimensionless shear stresses are:

• the upper/lower faces

$$(4.14) \qquad \overline{\tau}_{xy}^{(3,f)}(\xi,\eta) = \frac{9}{1+\nu_f} \frac{1-4\eta^2}{1+\beta} \left[1 - \frac{\cosh(k_3\lambda\xi)}{\cosh(k_3\lambda/2)}\right] \frac{C_{v\psi 3}}{C_{vv3}C_{\psi 3}}.$$

• the core

$$(4.15) \qquad \overline{\tau}_{xy}^{(3,c)}(\xi,\eta) = \frac{9}{1+\nu_c} C_0 \frac{1-(1-e_c)\chi_c^2 - 4e_c\eta^2}{1+\beta} \frac{e_0}{\chi_c}$$

$$\cdot \left[1 - \frac{\cosh(k_3\lambda\xi)}{\cosh(k_3\lambda/2)}\right] \frac{C_{v\psi 3}}{C_{vv3}C_{\psi 3}}.$$

4.2. *Elastic buckling of the beam*

Thus, the critical force of the beam (2.33) for the third model is as follows:

$$(4.16) \qquad F_{o,CR}^{(3)} = \overline{F}_{o,CR}^{(3)} E_f bh,$$

where the dimensionless critical force is

$$(4.17) \qquad \overline{F}_{o,CR}^{(3)} = \left(1 - C_{se,CR}^{(3)}\right) \frac{\pi^2 C_{vv3}}{12\lambda^2},$$

and the shear coefficient in the buckling is

$$(4.18) \qquad C_{se,CR}^{(3)} = \max_\beta \frac{\pi^2}{\pi^2 C_{\psi\psi 3} + \lambda^2 C_{\psi 3}} \frac{C_{v\psi 3}^2}{C_{vv3}}.$$

4.3. *Free flexural vibration of the beam*

Consequently, the fundamental natural frequency (2.41) for the third model is as follows:

$$(4.19) \qquad f_z^{(3)} = \frac{\omega^{(3)}}{2\pi} = \frac{\sqrt{3}\pi^2 10^6}{6\lambda^2} \sqrt{\left(1 - C_{se,fv}^{(3)}\right) C_{vv3} \frac{E_f}{\rho_b h^2}} \quad [\text{Hz}],$$

where the shear coefficient in the free flexural vibration $C_{se,fv}^{(3)} = C_{se,CR}^{(3)}$.

5. Exemplary analytical calculations – comparative analysis

Exemplary calculations are carried out for the following data of the sandwich beams: $E_f = 72000$ MPa, $\nu_f = 0.33$, $\rho_f = 2710$ kg/m^3, $E_c = 3600$ MPa, $\nu_c = 0.30$, $\rho_c = 610$ kg/m^3, $b = 18$ mm, $h = 20$ mm, $e_c = 1/20$, and $\lambda = 15$, 20, 25, 30. The results of the calculations are specified in Tables 1–6. The dimensionless shear stresses for the first model (2.26), (2.28), the second model (3.14), (3.15) and the third model (4.14), (4.15) of the exemplary beams for three-point bending are presented in Fig. 5.

- The value of the relative thickness of the core $\chi_c = 18/20$.

Table 1. The first model.

λ	15	20	25	30
$C_{se,b}^{(1)}$	0.0596384	0.0340247	0.0219594	0.0153345
$\overline{v}_{\max}^{(1)}$	193.867	336.323	519.373	743.049
$C_{se,CR}^{(1)}$	0.0489570	0.0282265	0.0182764	0.0127731
$\overline{F}_{o,CR}^{(1)}$	0.00106883	0.000614325	0.000397194	0.000277375
$f_z^{(1)}$ [Hz]	510.580	290.314	186.750	130.050

Table 2. The second model.

λ	15	20	25	30
$C_{se,b}^{(2)}$	0.0714646	0.0402602	0.0257901	0.0179207
$\overline{v}_{\max}^{(2)}$	196.031	338.351	521.320	744.941
$C_{se,CR}^{(2)}$	0.0558294	0.0321915	0.0208445	0.0145683
$\overline{F}_{o,CR}^{(2)}$	0.00106111	0.000611818	0.000396155	0.00027687
$f_z^{(2)}$ [Hz]	508.731	289.721	186.505	129.932

Table 3. The third model.

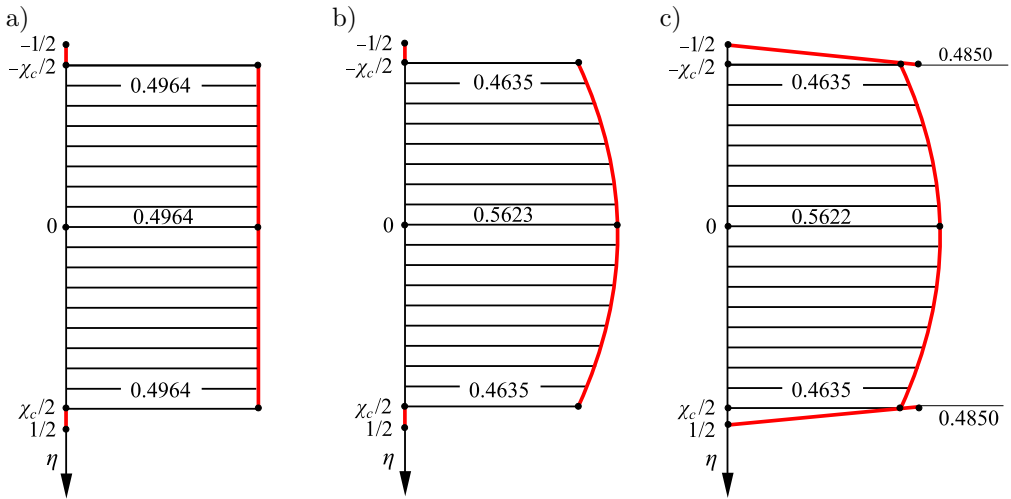| λ	15	20	25	30
β $C_{se,b}^{(3)}$	4.487 0.0715806	4.549 0.0403241	4.586 0.0258305	4.612 0.0179485
$\overline{v}_{\max}^{(3)}$	196.053	338.372	521.340	744.962
β $C_{se,CR}^{(3)}$	4.734 0.0559080	4.737 0.0322379	4.739 0.0208749	4.739 0.0145896
$\overline{F}_{o,CR}^{(3)}$	0.00106102	0.000611789	0.000396142	0.000276865
$f_z^{(3)}$ [Hz]	508.710	289.714	186.503	129.931

FIG. 5. Graphs of the dimensionless shear stresses for $\xi = 1/4$, $\lambda = 15$, $\chi_c = 18/20$:
a) first model, b) second model, c) third model.

- The value of the relative thickness of the core $\chi_c = 16/20$.

Table 4. The first model.

λ	15	20	25	30
$C_{se,b}^{(1)}$	0.105892	0.0603227	0.0388977	0.0271471
$\overline{v}_{\max}^{(1)}$	121.118	206.449	316.059	449.977
$C_{se,CR}^{(1)}$	0.083410	0.0488123	0.0318347	0.0223385
$\overline{F}_{o,CR}^{(1)}$	0.00172082	0.0010045	0.000654354	0.00045887
$f_z^{(1)}$ [Hz]	578.048	331.232	213.872	149.249

Table 5. The second model.

λ	15	20	25	30
$C_{se,b}^{(1)}$	0.116236	0.0656107	0.0420782	0.0292615
$\overline{v}_{\max}^{(1)}$	122.251	207.479	317.026	450.903
$C_{se,CR}^{(1)}$	0.0883291	0.0516923	0.0337135	0.0236570
$\overline{F}_{o,CR}^{(1)}$	0.00171159	0.00100145	0.000653085	0.000458251
$f_z^{(1)}$ [Hz]	576.496	330.730	213.664	149.148

Table 6. The third model.

λ	15	20	25	30
$C_{se,b}^{(1)}$	7.565 0.116748	7.672 0.0658930	7.737 0.0422568	7.780 0.0293845
$\overline{v}_{\max}^{(1)}$	122.307	207.534	317.061	450.957
$C_{se,CR}^{(1)}$	7.972 0.0886542	7.985 0.0518897	7.991 0.0338445	7.994 0.0237498
$\overline{F}_{o,CR}^{(1)}$	0.00171098	0.00100125	0.000652996	0.000458207
$f_z^{(1)}$ [Hz]	576.393	330.696	213.650	149.141

6. Exemplary FEM calculations – comparative analysis

The finite element model of the beam was built using the ABAQUS code. Because of the symmetry of the problem, only a quarter of the beam was used with proper boundary conditions in the symmetry planes. The beam geometry and loading are described in Fig. 6. It can be observed in Fig. 6 that the FE model has two symmetry planes perpendicular to the x-axis and z-axis, respectively. Loading is applied to the reference point at the centre of the top faces of the beam with the use of coupling constraints. The boundary conditions at the end of the beam are applied to the second reference point coupled with the planes of faces at the end of the beam. The faces and the core are modelled with the use of C3D8R solid elements. The convergence analysis has been made, and
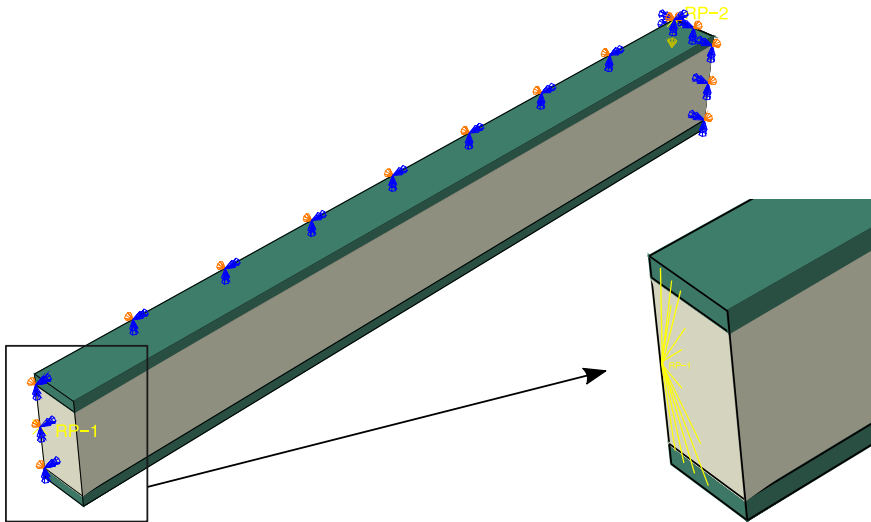

Fig. 6. The finite element model in ABAQUS.

it is observed that at least two elements are needed along the thickness of the face. Therefore the beam was discretised with a mesh size of 0.5 mm with no refinements. The results from the FEM analysis are collected in Tables 7–8.

Table 7. The results from the FEM model for the relative thickness of the core $\chi_c = 18/20$.

λ	15	20	25	30
$\overline{v}_{\max}^{(\text{FEM})}$	195.543	337.732	520.659	744.25
$\overline{F}_{o,CR}^{(\text{FEM})}$	0.0010693	0.00061421	0.00039699	0.00027719
$f_z^{(\text{FEM})}$ [Hz]	508.05	289.21	186.25	129.79

Table 8. The results from the FEM model for the relative thickness of the core $\chi_c = 16/20$.

λ	15	20	25	30
$\overline{v}_{\max}^{(\text{FEM})}$	122.149	207.369	316.949	450.915
$\overline{F}_{o,CR}^{(\text{FEM})}$	0.0017264	0.00100579	0.00065461	0.00045883
$f_z^{(\text{FEM})}$ [Hz]	575.67	330.21	213.39	148.98

For comparison purposes, the third model is considered as the reference model because, in this model, the full nonlinear shear effect is taken into account. The results obtained for the first, the second and the FEM models were compared with the third model ones for both cases of the relative thicknesses of the core. The percentage differences of the compared results are presented in Tables 9–14. The minus sign in front of the data in the tables below means that this result is underestimated in comparison to the third model result.

Table 9. The percentage difference between the first model and the third model for the relative thickness of the core $\chi_c = 18/20$.

λ	15	20	25	30
$\Delta\overline{v}_{\max}$	-1.12%	-0.61%	-0.38%	-0.26%
$\Delta\overline{F}_{o,CR}$	0.73%	0.41%	0.27%	0.18%
Δf_z [Hz]	0.37%	0.21%	0.13%	0.09%

Table 10. The percentage difference between the second model and the third model for the relative thickness of the core $\chi_c = 18/20$.

λ	15	20	25	30
$\Delta\overline{v}_{\max}$	-0.011%	-0.006%	-0.004%	-0.003%
$\Delta\overline{F}_{o,CR}$	0.008%	0.005%	0.003%	0.002%
Δf_z [Hz]	0.004%	0.002%	0.001%	0.001%

Table 11. The percentage difference between the FEM model and the third model for the relative thickness of the core $\chi_c = 18/20$.

λ	15	20	25	30
$\Delta\overline{v}_{\max}$	-0.26%	-0.19%	-0.13%	-0.10%
$\Delta\overline{F}_{o,CR}$	0.78%	0.39%	0.21%	0.12%
Δf_z [Hz]	-0.13%	-0.17%	-0.14%	-0.11%

Table 12. The percentage difference between the first model and the third model for the relative thickness of the core $\chi_c = 16/20$.

λ	15	20	25	30
$\Delta\overline{v}_{\max}$	-0.98%	-0.52%	-0.32%	-0.22%
$\Delta\overline{F}_{o,CR}$	0.57%	0.32%	0.21%	0.14%
Δf_z [Hz]	0.29%	0.16%	0.10%	0.07%

Table 13. The percentage difference between the second model and the third model for the relative thickness of the core $\chi_c = 16/20$.

λ	15	20	25	30
$\Delta\overline{v}_{\max}$	-0.046%	-0.027%	-0.011%	-0.012%
$\Delta\overline{F}_{o,CR}$	0.036%	0.020%	0.014%	0.010%
Δf_z [Hz]	0.018%	0.010%	0.007%	0.005%

Table 14. The percentage difference between the FEM model and the third model for the relative thickness of the core $\chi_c = 16/20$.

λ	15	20	25	30
$\Delta\overline{v}_{\max}$	-0.13%	-0.08%	-0.04%	-0.01%
$\Delta\overline{F}_{o,CR}$	0.90%	0.45%	0.25%	0.14%
Δf_z [Hz]	-0.13%	-0.15%	-0.12%	-0.11%

7. Conclusions

The detailed analytical analysis shows that considering the nonlinear shear effect has a significant impact on the obtained values. The results for the first analytical model show that the "broken line" theory gives the lower deflection and higher critical load and fundamental natural frequency in comparison to the third model. The differences between results obtained for the second and third model for the considered cases of relative thickness are negligible. Therefore, for the classical sandwich beam with thin faces, the shear effect in the faces can be

neglected. For considered cases of the beam geometry, the maximum percentage difference between the FEM model and the third model, which is treated as the reference model, is 0.9% for the critical load, -0.17% for the fundamental natural frequency and -0.26% for the beam deflection. The comparisons between the results for the third and FEM models prove that the critical load, the fundamental natural frequency and the maximum deflection given by the developed analytical formulas are in excellent agreement with the ones obtained from the FEM.

References

1. PLANTEMA F.J., *Sandwich Construction: The Bending and Buckling of Sandwich Beams, Plates, and Shells*, John Wiley & Sons, Inc., New York, London, Sydney, 1966.

2. ALLEN H.G., *Analysis and Design of Structural Sandwich Panels*, Pergamon Press, Oxford, London, Edinburgh, New York, Toronto, Sydney, Paris, Braunschweig, 1969.

3. NOOR A.K, BURTON W.S., BERT C.W., Computational models for sandwich panels and shells, *Applied Mechanics Reviews*, **49**(3): 155–199, 1996, doi: 10.1115/1.3101923.

4. FROSTIG Y., Buckling of sandwich panels with a flexible cores – high-order theory, *International Journal of Solids and Structures*, **35**(3–4): 183–204, 1998, doi: 10.1016/S0020-7683(97)00078-4.

5. VINSON J.R., Sandwich structures, *Applied Mechanics Reviews*, **54**(3): 201–214, 2001, doi: 10.1115/1.3097295.

6. ICARDI U., Applications of Zig-Zag theories to sandwich beams, *Mechanics of Advanced Materials and Structures*, **10**(1): 77–97, 2003, doi: 10.1080/15376490306737.

7. STEEVES C.A., FLECK N.A., Collapse mechanisms of sandwich beams with composite faces and a foam core, loaded in three-point bending. Part 1: analytical models and minimum weight design, *International Journal of Mechanical Sciences*, **46**(4): 561–583, 2004, doi: 10.1016/j.ijmecsci.2004.04.003.

8. YANG M., QIAO P., Higher-order impact modeling of sandwich structures with flexible core, *International Journal of Solids and Structures*, **42**(20): 5460–5490, 2005, doi: 10.1016/j.ijsolstr.2005.02.037.

9. MAGNUCKA-BLANDZI E., MAGNUCKI K., Effective design of a sandwich beam with a metal foam core, *Thin-Walled Structures*, **45**(4): 432–438, 2007, doi: 10.1016/j.tws.2007.03.005.

10. CARRERA E., BRISCHETTO S., A survey with numerical assessment of classical and refined theories for the analysis of sandwich plates, *Applied Mechanics Reviews*, **62**(1): 010803, 2009, doi: 10.1115/1.3013824.

11. KREJA I., A literature review on computational models for laminated composite and sandwich panels, *Central European Journal of Engineering*, **1**(1): 59–80, 2011, doi: 10.2478/s13531-011-0005-x.

12. MAGNUCKA-BLANDZI E., Dynamic stability and static stress state of a sandwich beam with a metal foam core using three modified Timoshenko hypothesis, *Mechanics of Advanced Materials and Structures*, **18**(2): 147–158, 2011, doi: 10.1080/15376494.2010.496065.

13. MAGNUCKA-BLANDZI E., Mathematical modelling of a rectangular sandwich plate with a metal foam cores, *Journal of Theoretical and Applied Mechanics*, **49**(2): 439–455, 2011.

14. BABA B.O., Free vibration analysis of curved sandwich beams with face/core debond using theory and experiment, *Mechanics of Advanced Materials and Structures*, **19**(5): 350–359, 2012, doi: 10.1080/15376494.2010.528163.

15. PHAN C.N., FROSTIG Y., KARDOMATEAS G.A., Analysis of sandwich beams with a compliant core and with in-plane rigidity–extended high-order sandwich panel theory versus elasticity, *ASME: Journal of Applied Mechanics*, **79**(4): 041001–1-11, 2012, doi: 10.1115/1.4005550.

16. MAGNUCKI K., JASION P., SZYC W., SMYCZYNSKI M., Strength and buckling of a sandwich beam with thin binding layers between faces and a metal foam core, *Steel and Composite Structures*, **16**(3): 325–337, 2014, doi: 10.12989/scs.2014.16.3.325.

17. SAYYAD A.S., GHUGAL Y.M., Bending, buckling and free vibration of laminated composite and sandwich beams: a critical review of literature, *Composite Structures*, **171**: 486–504, 2017, doi: 10.1016/j.compstruct.2017.03.053.

18. MAGNUCKA-BLANDZI E., Bending and buckling of a metal seven-layer beam with crosswise corrugated main core – Comparative analysis with sandwich beam, *Composite Structures*, **183**: 35–41, 2018, doi: 10.1016/j.compstruct.2016.11.089.

19. CZECHOWSKI L., JANKOWSKI J., KOTEŁKO M., JANKOWSKI M., Experimental and numerical three-point bending test for sandwich beams, *Journal of KONES Powertrain and Transport*, **24**(3): 53–62, 2017, doi: 10.5604/01.3001.0010.3071.

20. BIRMAN V., KARDOMATEAS G.A., Review of current trends in research and applications of sandwich structures, *Composites Part B: Engineering*, **142**: 221–240, 2018, doi: 10.1016/j.compositesb.2018.01.027.

21. SAYYAD A.S., GHUGAL Y.M., Modeling and analysis of functionally graded sandwich beams: A review, *Mechanics of Advanced Materials and Structures*, **26**(21): 1776–1795, 2019, doi: 10.1080/15376494.2018.1447178.

22. ZHEN W., YANG C., ZHANG H., ZHENG X., Stability of laminated composite and sandwich beams by a Reddy-type higher-order zig-zag theory, *Mechanics of Advanced Materials and Structures*, **26**(19): 1622–1635, 2019, doi: 10.1080/15376494.2018.1444228.

23. MAGNUCKI K., Bending of symmetrically sandwich beams and I-beams – analytical study, *International Journal of Mechanical Sciences*, **150**: 411–419, 2019, doi: 10.1016/j.ijmecsci.2018.10.020.

24. Magnucki K., Magnucka-Blandzi E., Generalization of a sandwich structure model: Analytical studies of bending and buckling problems of rectangular plates, *Composite Structures*, **255**: 112944, 2021, 112944, doi: 10.1016/j.compstruct.2020.112944.

────────